Determination of Lanthanides in Fossil Samples Using Laser Induced Breakdown Spectroscopy

[1]Jesús-Manuel Anzano[*], [1]Jaime Cajal, [1]Roberto-Jesús Lasheras, [2]Miguel Escudero, [3]Ignacio Canudo
[4]Mariano Laguna, and [5]Jamil Anwar
[1]*Laser Laboratory and Environment, Department of Analytical Chemistry, Faculty of Sciences, University of Zaragoza, Zaragoza, Spain.*
[2]*Centro Universitario de la Defensa (CUD) de Zaragoza, Zaragoza, Spain.*
[3]*Department of Sciences of Earth, Faculty of Sciences, IUCA, University of Zaragoza, Zaragoza, Spain.*
[4]*Department of Inorganic Chemistry, ISQCH, University of Zaragoza, Zaragoza, Spain.*
5School of Physical Sciences, University of the Punjab, Lahore, PAKISTAN.
janzano@unizar.es*

(Received on 17th June 2016, accepted in revised form 30th May 2017)

Summary: As being a fast, simple and relatively non-destructive analytical technique Laser-induced breakdown spectroscopy (LIBS) has a large variety of applications including the analysis of paleontological samples. In this work LIBS is employed for the quantitative determination of lanthanides (Ce, Dy, Er, Eu, Gd, Ho, La, Lu, Nd, Sm, Tb, Tm and Yb) in vertebrate fossil samples comprising teeth, disarticulated complete or fragmented bones, eggshell fragments, and coprolites of dinosaurs, mammals and crocodiles. For emission line data, standard AnalaR grade salts of lanthanides were used. The major components: iron, calcium, magnesium, silicon and aluminum in the samples were also determined. The analytical information may be helpful in studying the samples for their age, formation environment and other paleontological properties.

Keywords: Laser Induced Breakdown Spectroscopy; LIBS; lanthanides; Fossil analysis.

Introduction

Laser induced breakdown spectroscopy [LIBS] is an effective and powerful optical emission spectroscopic analytical technique capable of analyzing a large variety of samples. It is equally useful for research and industrial applications. Though it is relatively a new technique in the field of analytical chemistry yet it has been frequently employed for industrial, environmental, agricultural and geological samples. Other than elemental analysis, this technique has also been used for surface studies and other material properties of solids. LIBS was originated as a qualitative analytical tool but the developments in recent years proved it a reliable technique for quantitative analysis. The two major advantages of LIBS are its speed and little use of sample. Due to the negligible consumption of sample during analysis the technique can be considered as a semi non-destructive technique. The sample loss during LIBS analysis is usually in the range of nanogram to microgram [1].

Practically, a high power density beam of pulsed radiation from a laser source is focused on a small area of the sample. Due to high energy of laser radiation, a small amount of the sample, usually from few picograms to few nanograms is ablated and generates a plasma plume with temperatures exceeding from 10^5K. At this high temperature the specimen material dissociates into ions, atoms, molecules and free electrons. At initial stages of plasma formation and dissociation, when the temperature is very high, a continuum of radiation is emitted, which is usually of no analytical use. However after a few microseconds the temperature falls in the range of $5x10^3$K to $2x10^4$K. At this stage the characteristic atomic emission lines from the elements can be observed. The delay between the emission of continuum radiation and characteristic radiation is in the order of 10 micro seconds or less this is why it is necessary to use a gate detector to capture the desired spectrum. Spectroscopic analysis of the emitted radiation from the excited plasma enables identification and quantification of the elements present in sample.

For accurate quantitative determination at microgram level analytical emission intensity data of the analytes has to be stored in the machine before the actual analysis. This can be done by employing standards of the elements needed to be analyzed. LIBS is not free from problems and limitations. Two major problems, mostly encountered in this technique, are matrix effects and spectral interferences. These difficulties are usually faced in the case of high-density multielemental samples. These problems, however, can be eliminated by using high-resolution monochromator fitted with a boxcar-integrated gateway [2].

Multi-element analysis of complex samples with adequate accuracy is one of the outstanding properties of LIBS. Using laser induced breakdown spectroscopy, we have analyzed polymers [3-5],

[*]**To whom all correspondence should be addressed.**

archaeological [6-7], geological [8, 9], soils [10] and biological [11-12] samples.

Accurate composition of fossils, up to elements present in them at nanogram levels, always provides valuable information for ascertaining their age, environment of their formation and other paleontological properties. Determination of lanthanides by any physio-chemical technique is a always a difficult task due to the similarity in their chemical and physical behavior. In this work lanthanides (Ce, Dy, Er, Eu, Gd, Ho, La, Lu, Nd, Sm, Tb, Tm and Yb)are quantitatively determined by using LIBS in vertebrates fossil samples comprising teeth, disarticulated complete or fragmented bones, eggshell fragments, and coprolites of dinosaurs, mammals, crocodiles. The Department of Earth Sciences and Paleontology, University of Zaragoza, Spain has provided the fossil samples (Fig. 1). These samples were collected from the site of La Cantalera, Spain. To date, 31 different vertebrate taxa have been identified [13-15].

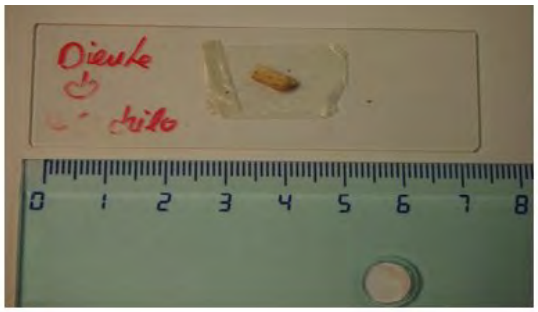

M1: Crocodile tooth

M2: Crocodile tooth

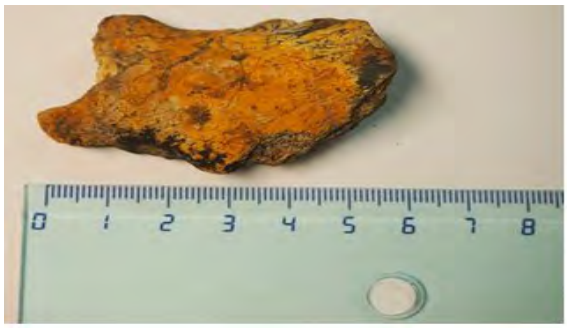

M3: Indeterminate 1

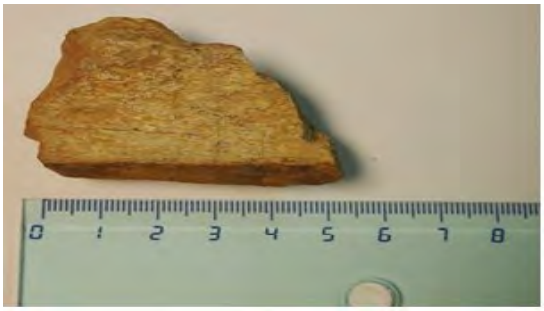

M4: Indeterminate 2

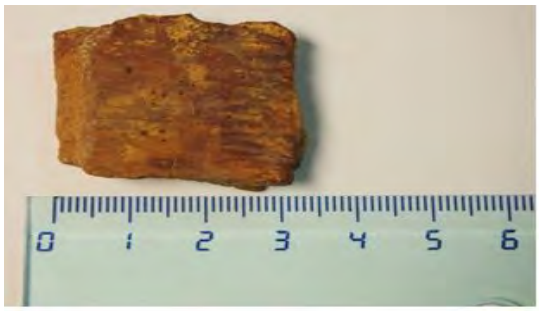

M5: Tortoise

M6: Tortoise 1

Fig. 1: Real Fossil Samples.

Experimental

Samples and Standard Preparation

The reagents used as standards in this work consist of a series of lanthanide salts, were of highest purity obtained from AnalaR Grade, Sigma-Aldrich; Merck and other International Chemical Suppliers. Following salts of lanthanides were used as standards: Samarium (III) chloride hexahydrate, Lanthanum (III) nitrate hexahydrate, Europium (III) nitrate hexahydrate, Terbium (III) nitrate hexahydrate, Holmium(III) nitrate hydrate, Thulium (III) nitrate hexahydrate, Lutetium (III) nitrate hexahydrate, Erbium (III) nitrate hexahydrate, Samarium (III) nitrate hexahydrate, Neodymium (III) nitrate hexahydrate, Gadolinium (III) nitrate hexahydrate, Dysprosium (III) nitrate pentahydrate, Ytterbium (III) nitrate pentahydrate, and Cerium (III) nitrate hexahydrate. Spectroscopy grade potassium bromide was used as "diluent".AnalaR Grade salts of iron, calcium, magnesium, silicon and aluminum were used as the standards of major elements.

The standard salts and the sample was homogenized for 5 minutes manually in a aggrade pestle and mortar. The fine powder was pressed into pellets using a manual hydraulic press under a pressure of 10000 kPa for 5 min. The pellet size was 12mm in diameter and about 1 mm in thickness.

Instrumental Setup

Each sample was exposed to laser beam of 1064 nm (pulse width 7.7 ns and a maximum pulse energy 50 mJ at 1064 nm) originated from a Q-switched Nd:YAG laser (Quantel, model Ultra CFR) and focused through a 150 mm focal length lens.The target surface was positioned approximately 70 mm above the focal plane to avoid break down in air and the resulting laser spot diameter was d ≈ 1mm. The emitted radiation from the laser plasma was collected with a bifurcated optical fiber (QBIF600-UV-VIS, 600um, Premium Bifurcated Fiber, UV/VIS, 2m, ATO) connected to a dual-channel Ocean-Optics spectrometer (LIBS2500plus, Ocean Optics Inc., Dunedin, FL, USA). Plasma spectrum was collected in a non-collinear mode. The pulse energy employed was 25 mJ approximately, because using a higher energy than this value caused saturation in emission lines. The position of the collimating lens (74-UV Ocean Optics, f/2 fused silica lens for 200–2000 nm, 5 mm diameter, 10 mm focal length) was adjusted for maximum light collection at 45º with respect to the sample surface. The settings of spectrometer were as follows: Channel one, HR2000+ grating H5, select 205-220 nm, best: 200-400 nm, DET2B-UV ILX-511B detector, with UV2 window and optical bench entrance aperture, 10-micron width; and Channel two: HR2000+ Grating H3, select 410-440 nm, best: 350-850 nm, DET2B-VIS ILX-511B detector with VIS window, optical bench entrance aperture, 10-micron width, and F1-GG395longpass filter (transmits >395 nm). In order to optimize the experimental conditions like: signal-to-noise ratio, atomic lines FWHM and spectral interference a delay time of 2.5 μs with respect to the laser pulse and a gate time of 10 μs were adjusted. The delay time was sufficient to suppress background signals from continuum plasma radiation. The spectrometer is triggered to acquire and read out data simultaneously. The optimized experimental parameters for laser pulse energy, gate delay time, gate width, number of average shot spectra are fixed for all experimental data acquisition procedures.

Each sample measurement consisted of 5 replicas; one replica is the average of 50 laser shots per measurement using an average delay of 100ms between the scans. Hence two hundred and fifty LIBS spectra were recorded for each sample.

Results and discussion

Choice of Analytical Lines

Though Laser Induced Breakdown Spectroscopy has the capability of simultaneous multi-element analysis but at the same time there is every possibility of false results due to spectral interferences if the working emission lines are not chosen carefully. Emission due to ionic and molecular species as well as self-absorption also becomes serious interfering factors in certain cases. The effect of self-absorption weakens the intensity of the lines and elemental abundance is underestimated. This is particularly true for major elements for which non-linear effects are significant. Hence choice of analytical lines for a particular item is always a crucial step in LIBS. Usually to avoid the spectral interference and self- absorption, two considerations are kept in view prior to selection of a working line for an element. First is that too close lines are usually avoided, for example Fe (373.51 nm) and Mg (373.52 nm); hence Fe was measured at (299.9 nm). Same strategy was adopted in the case of other elements. Secondly, in order to reduce self-adsorption, the lines terminating in a heavily populated level, such as resonant lines were avoided. Therefore iron lines of (271.9 nm) and (282.5 nm) were avoided in this work. Nevertheless, some resonant lines such as Ca (393.3 nm) and Ca (396.7 nm), Mg (285.2 nm), and Mg (279.5 nm) have been chosen to study their behaviour. The wavelengths of the spectral lines studied throughout this work are shown in Table-1.

Table-1: Workable Emission (atomic) lines of Lanthanides.

Element	Emission Lines (nm)
Calcium	**316.06 (d), 317.82 (m), 370.83 (d), 373.6 (d), 393.26 (f), 369.69 (f)**
Iron	**254.1 (d), 274.71 (f), 300.21 (d), 322.70 (d), 358.00 (m), 374.29 (m), 381.89 (m), 404.59 (d), 406.30 (d)**
Magnesium	**279.69 (m), 285.36 (d), 293.50 (d), 382.93 (f)**
Aluminium	**309.03 (m), 358.35 (m), 394.28 (m), 396.01 (f)**
Silicon	**288.16(m)**
Cerium	**365.58 (m), 380.15 (m), 394.27 (f), 407.58(f), 418.65 (f)**
Dysprosium	**321.66 (f), 340.77(f), 357.62(f), 364.53(f)**
Erbium	**323.05 (f), 349.91 (f), 369.26(f), 390.63 (m)**
Europium	**352.11(m), 368.84 (f), 381.96(f), 390.71(f), 393.04 (f)**
Gadolinium	**303.28 (m), 336.22 (f), 342.24 (f), 348.12 (f), 364.60(m), 376.7 (f)**
Holmium	**308.43 (m), 317.37 (m), 339.89 (m), 345.60 (a), 388.89 (f)**
Lanthanum	**357.44 (m), 379.47 (f), 394.91 (a), 404.29 (m)**
Lutetium	**364.77 (m), 384.11 (m), 412.47 (m), 451.85 (m), 513.50(f), 547.66(f)**
Neodymium	**378.42 (m), 380.53(m), 390.02 (f), 401.22 (m), 406.10 (m)**
Samarium	**330.63(m), 356.82 (f), 359.26 (f)**
Terbium	**431.88 (f), 432.64(f), 433.84 (f)**
Thulium	**323.68 (m), 326.66 (a), 346. 22 (f)**
Ytterbium	**328.93 (f),369.41(f)**

(d = weak intensity; m =medium intensity; f =strong intensity)

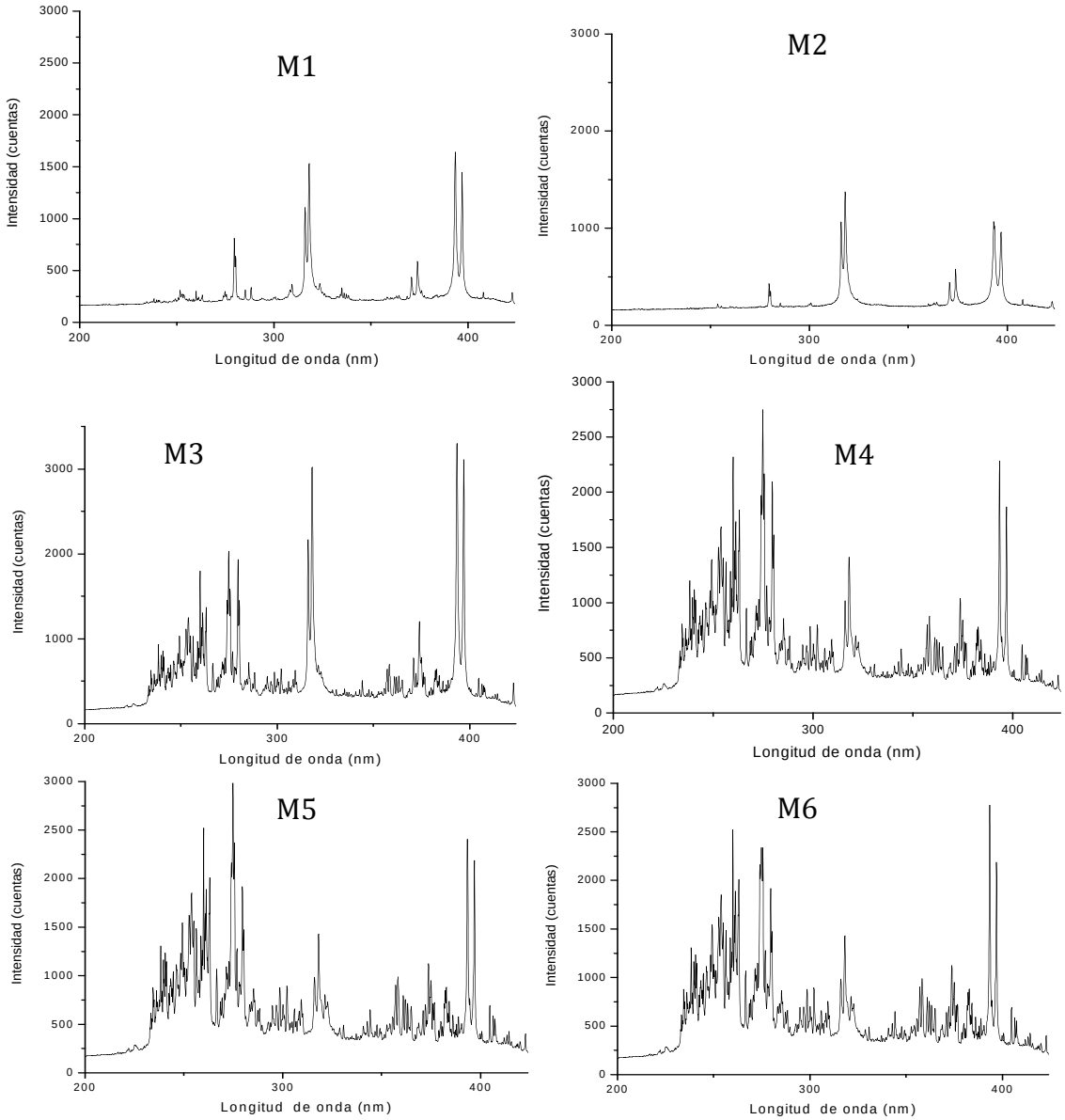

Fig. 2: LIBS spectra of samples of fossils.

Qualitative Analysis of Fossil Material

The LIBS spectra of the fossil samples analyzed in this work are shown in Fig. 2. A careful observation of the spectra reveals that samples belonged to two groups. The samples M1, M2 and M5 can be placed in first group and samples M3, M4 and M6 can be classified as members of second group. Spectra of the samples within a group closely resemble with each other. As spectra indicate the presence of different elements in the sample hence this can be safely said that chemical composition of members in each group is identical.

Qualitative studies showed that all the six samples without exception contain sufficient amounts of calcium as every spectrum showed its line. Half of the samples, marked M1, M2 and M5 did not show the presence of iron while the spectra of samples designated as M3, M4 and M6 clearly indicated that iron was present. Like calcium, all the samples contained significant amounts of magnesium and silicon. Similarly, all except one (M1) showed the presence of aluminum.

As far as the presence of lanthanides in fossil materials was concerned, gadolinium has been found in all the samples except one (M5). Europium had been found in half of the samples (M3, M4 and M6), while the other specimens did not show the presence of this element. Only two samples (M1 & M2) contained samarium while lanthanum was present in M4 and M6. Neodymium was found only in M3, M4 and M6 samples. None of the fossil samples contained any other element of lanthanide series except those mentioned above. Elements detected in various fossil samples are shown in Table 2.

Table-2: Qualitative analysis of the fossil samples.

Element	M1	M2	M3	M4	M5	M6
Calcium	Yes	Yes	Yes	Yes	Yes	Yes
Iron	No	No	Yes	Yes	No	Yes
Magnesium	Yes	Yes	Yes	Yes	Yes	Yes
Silicon	Yes	Yes	Yes	Yes	Yes	Yes
Aluminum	No	Yes	Yes	Yes	Yes	Yes
Lanthanum	No	No	No	Yes	No	Yes
Cerium	No	No	No	No	No	No
Neodymium	No	No	Yes	Yes	No	Yes
Samarium	Yes	Yes	No	No	No	No
Europium	No	No	Yes	Yes	No	Yes
Gadolinium	Yes	Yes	Yes	Yes	No	Yes
Terbium	No	No	No	No	No	No
Dysprosium	No	No	No	No	No	No
Holmium	No	No	No	No	No	No
Erbium	No	No	No	No	No	No
Thulium	No	No	No	No	No	No
Ytterbium	No	No	No	No	No	No
Lutetium	No	No	No	No	No	No

Table-3: Analytical Data for Calibration of lanthanides.

Element	Emission Line	Data
Cerium	365.6 nm	y = 39,62x – 6,21 R² = 0,9991
	394.3 nm	y = 51,05x + 10,40 R² = 0,9855
	407.5 nm	y = 46,37x + 6,22 R² = 0,9999
	418.7 nm	y = 17,30x + 2,27 R² = 0,9685
Gadolinium	303.2 nm	y = 4,66x + 12,85 R² = 0,9592
	310.0 nm	y = 9,94x + 35,84 R² = 0,9964
	336.1 nm	y = 6,88x + 42,53 R² = 0,9762
	342.2 nm	y = 15,11x + 41,28 R² = 0,9865
	348.1	y = 7,27x + 26,84 R² = 0,9836
Europium	368.8 nm	y = 31,19x + 7,88 R² = 0,9996
	381.9 nm	y = 239,52x + 142,83 R² = 0,9894
	390.7 nm	y = 118,87x + 40,90 R² = 0,9947
	393.0 nm	y = 139,18x + 55,91 R² = 0,9947
Neodimium	378.4 nm	y = 31,87x + 12,12 R² = 0,9750
	380.6 nm	y = 25,42x + 5,20 R² = 0,9741
	389.0 nm	y = 42,04x + 14,29 R² = 0,9562
	401.3 nm	y = 45,67x + 24,81 R² = 0,9686
Samarium	356.8 nm	y = 15,44x + 44,43 R² = 0,9843
	359.2 nm	y = 19,14x + 61,79 R² = 0,9809

Characterization of the Plasma

The temperature of the plasma produced was determined by using Boltzmann plot method. While LTE is established within the plasma, the population at different levels is governed by the Boltzmann distribution law. This law correlates the line intensity for the given transition $E_k \rightarrow E_i$ of an atomic specie, as shown by the Eq. (1)

$$\ln\frac{I_{\lambda}^{ki}}{A_{ki}g_k} = -\frac{E_k}{k_B T} + \ln\frac{hcN(T)}{4\pi U(T)} \qquad (1)$$

In this equation I is the intensity of spectral line, A_{ki} and g_k are the transition probability and the statistic weight, respectively of the upper energy level labeled Ek, whereas k_B and h are the Boltzmann and Planck constants, respectively, c is the velocity of the light, and N and U(T) are total density of emitting species and partition function, respectively. As calcium was present in all samples therefore Ca (II) lines were used for temperature measurement using the standard Boltzman method. The relationship given in Eq.1 leads to a linear plot against E_k if several transitions of the same species are considered. The temperature of this species can be deduced from the slope of such a plot.

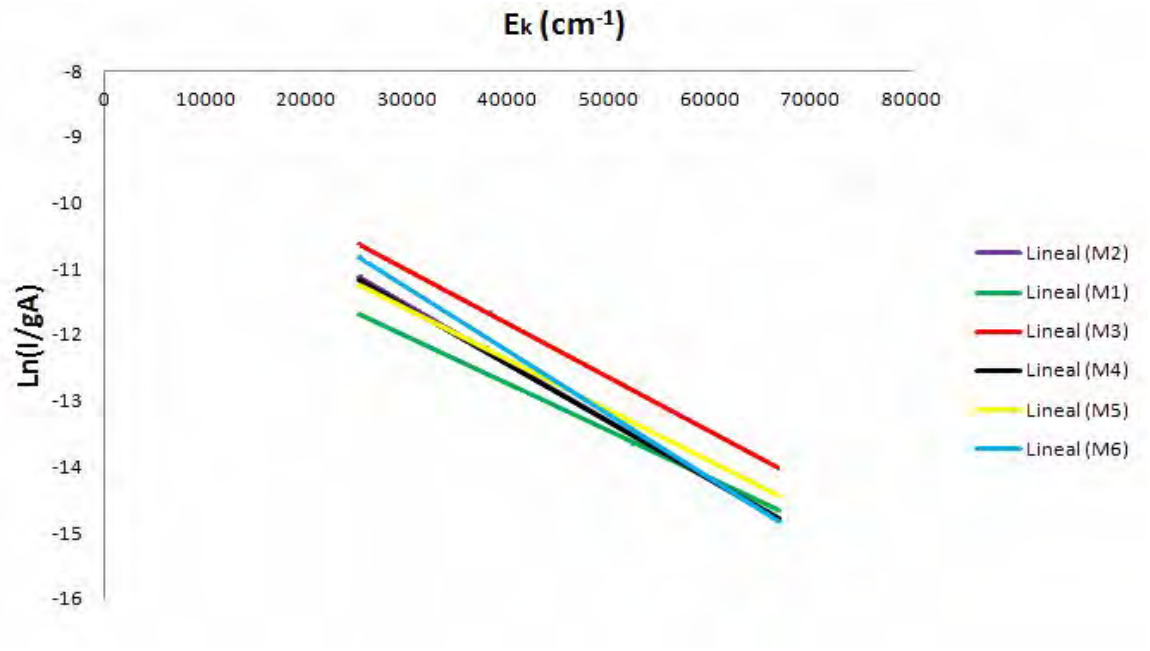

Fig. 3: Representation of the Boltzmann equation for the samples, Ca (II).

The temperature obtained in case of each sample is between 15000 and 20000 K. As shown in Fig. 3 slopes obtained in all cases are similar, indicating almost similar temperature in all cases, with a mean value of 17425 ± 1692 K. In plasma source the line-width is mainly due to Stark broadening, which results from the collisions of charged species [5], whereas Pressure and Doppler broadenings are quite small. The electron density was calculated from the Stark broadening of Ca (II) at 393.3 nm for the M1 sample.

The observed line-width, FWHM ($\Delta\lambda_{obs}$), have been corrected by subtracting the instrumental width ($\Delta\lambda_{inst}$) whose value is 0.1 nm for the spectrometer used. The corrected value obtained was 0.639 nm[4].The electron density (N_e), related to the full width at half maximum (FWHM) $\Delta\lambda$ of the stark broadened line is shown in Eq. (2).

$$N_e = \frac{\Delta\lambda \times 10^{16}}{2w} \left[cm^{-3}\right] \qquad (2)$$

where $\Delta\lambda$ is FWHM and w is the electron impact parameter which can be obtained corresponding to different plasma temperatures. The electron density calculated using (2) was 1.77×10^{17}MeV. The McWhirter criterion that provides the lowest value of the electron density necessary for the plasma to reach the LTE condition of local thermal equilibrium (LTE) requires verifying Eq. (3).

$$N_e \geq 1.6\times10^{12} T^{1/2} \Delta E^3 \qquad (3)$$

where N_e (cm^{-3}) is the electron density, T (K) is the plasma temperature, and ΔE (eV) is the largest energy transition. According to this criterion, if the largest energy (ΔE) is 6.61×10^{15}eV and the plasma temperature is 17000 ± 1700 K, Eq. (3) results in a minimal electron density value of $N_e = 1.77\times10^{17}$eV. The electron density obtained from Eq. (2) is greater than its respective lower limit given by Eq. (3), so the condition for LTE is fulfilled [4].

Calibration Curves

Calibrations (Sm, Eu, Gd, Nd and Ce) were carried out by using internal standards of these lanthanides which were diluted with potassium bromide. In most of the calibrations the higher levels of concentration is eliminated, since it is not a linear increase in the peak intensity, but less than the expected signal, this effect can be explained by the effect of self-absorption as explained observed previously and it is higher at high concentrations. To eliminate the inter-elemental interferences, multivariate calibrations were employed for quantitative work in most of the cases. The limit of detection was calculated by: Eq. (3)

$$LOD = 3\sigma/s \qquad (3)$$

where σ is the standard deviation of the background and s is the calibration slope. The limit of detection (LOD) of Ce, Eu, Gd, Nd y Sm are indicated in Table-4.

Table-4: Lanthanide concentrations obtained for each simple ([1] LD: Limit of detection; [2]Detected but below the lowest calibration level).

	Europium	Gadolinium	Neodimium	Samarium	Cerium
λ (nm)	368.8 nm	336.1[3] o 348.1[4] nm	378.4 nm	356.8 nm	365.3 nm
LD[1]:	0.03%	0.14%	0.05%	0.12%	0.03%
M1	Below L.D	0.47± 0.11%[3]	Below L.D.	Detected[2]	Below L.D
M2	Below L.D	1.33 ± 0.10%[3]	Below L.D.	Detected [2]	Below L.D
M3	1.44 ± 0.15 %	0.47 ± 0.14%[4]	1.24 ± 0.14 %	Below L.D	Below L.D
M4	1.40 ± 0.22 %	1.50 ± 0.16 %[4]	1.97 ± 0.17 %	Below L.D	Below L.D
M5	Below L.D	Below L.D	Below L.D.	Below L.D	Below L.D
M6	1.70 ± 0.11 %	1.70 ± 0.13 %[4]	2.40 ± 0.16 %	Below L.D	Below L.D

Quantitative Analysis

Finally, this calibration was used for the determination of Sm, Gd, Eu and Nd in fossil samples. Although the calibration was available for cerium also but this element was not detected in any of the samples analyzed in this work. There is every possibility that Ce may be present less than the limit of detection.

Europium was determined in M3, M4 and M6 samples as it was not detected in samples M1, M2 and M5 .The Eu was determined by using its emission line of 368.8 nm. It was found in the range of 1.4-1.7%. As shown in the table it was found in M3 (1.44 ± 0.15%), M4 (1.40 ± 0.22%) and M6 (1.70 ± 0.11%). Likewise Gadolinium, present in the samplesM1, M2, M3, M4 and M6 samples was determined by using the line 336.1 nm. It was not detected in M5. The concentrations obtained were M1 (0.47 ± 0.11%) and M2 (1.33 ± 0.10%). Due to spectral interference M3, M4 and M6 samples were analysed by using 348.1 nm emission lines. The results obtained for Gd in these samples were M3 (0.47 ± 0.14%) M4 (1.50 ± 0.16%) and M6 (1.70 ± 0.13%).

Neodymium was determined in M3, M4 and M6 samples as it was not detected in M1, M2 and M5 samples. The concentrations obtained, using emission line of 378.4 nm, were: M3 (1.24 ± 0.14%) M4 (1.97 ± 0.17%) and M6 (2.40 ± 0.16%). Samarium was detected in samples M1 and M2, but could not be quantified as being below the calibration range. A summary of the quantitative results of lanthanides is given in Table-5.

Table-5: Analytical Data for iron, calcium, and magnesium.

Element	Calibration curve	r
Fe λ (nm)		
266.4	y = 304.7x + 637.5	0.700
298.4	y = 290.8x + 536.2	0.724
340.7	y = 172.5x + 280.2	0.815
343.9	y = 349.9x + 380.7	0.317
375.8	y = 229.5x + 463.0	0.687
404.5	y = 252.2x + 368.8	0.805
Ca λ (nm)		
317.9	y = 95.37x + 378.8	0.777
393.3	y = 68.89x + 657.7	0.622
396.7	y = 75.56x + 347.3	0.649
445.8	y = 137.6x + 462.9	0.657
Mg λ (nm)		
279.5	y = -2849x + 940.2	0.783
285.2	y = 25115x +798.5	0.842
293.6	y = 3649x + 501.2	0.508

Conclusions

In this work LIBS has been used for the detection as well as quantitative determination of lanthanides in fossil samples collected from the site of Cantalera (Teruel). A database of spectral emission lines of lanthanides was prepared by using standard salts. Using these data base fossil samples was successfully analyzed qualitatively as well as quantitatively. The results obtained may be helpful for further paleontological work on these samples.

Acknowledgements

This work was supported by the Department of Innovation, Research and University of the Aragon Regional Government and the European Social Found (group E75), the University of Zaragoza (proposal #UZ2015-CIE-01) and General Services Research Support -SAI of University of Zaragoza.

Reference

1. S. Musazzi and U. Perini, *Laser-Induced Breakdown Spectroscopy: Theory & Applications*, Springer Series in Optical Sciences, Springer-Verlag Berlin, Heidelberg (2014).
2. D. A. Cremers, L. J. Radzimski, *Handbook of Laser Induced Breakdown Spectroscopy* (Ed.). John Wiley & Sons, England (2006).
3. R. J. Lasheras, C. Bello-Gálvez, E. M. Rodríguez-Celis and J. Anzano, Discrimination of Organic Solid Materials by LIBS Using Methods of Correlation and Normalized Coordinates, *J. Hazard. Mater.*, **192**, 704 (2011).
4. J. Anzano, B. Bonilla, B. Montull-Ibor and J. Casas, Plastic Identification and Comparison by Multivariate Techniques with Laser-Induced Breakdown Spectroscopy, *J. Appl. Polym. Sci.*, **121**, 2710 (2011).

5. R. J. Lasheras, C. Bello-Gálvez and J. Anzano, Identification of Polymers by Libs Using Methods of Correlation and Normalized Coordinates, *Polym. Test.,* **29**, 1057 (2010).
6. J. Anzano, S. Sangüesa, J. Casas-González, M. Á. Magallón, M. Escudero, J. Anwar and U. Shafique, Analysis of Roman-Hispanic Archaeological Ceramics using Laser-Induced Breakdown Spectroscopy, *Anal. Lett.,* **48**, 1638 (2015).
7. J. Anzano, R. Lasheras, E. Cunya, B. Bonilla, J. M. Begueria and J. Casas-Gonzalez, Analysis of Pre-Hispanic Archaeological Samples using Laser-Induced Breakdown Spectroscopy (LIBS), *Anal. Lett.*, **42**, 1509 (2009).
8. J. M. Anzano, M. A. Villoria, A. Ruiz-Medina and R. J. Lasheras, Laser-Induced Breakdown Spectroscopy for Quantitative Spectrochemical Analysis of Geological Materials: Effects of the Matrix and Simultaneous Determination, *Anal. Chim. Acta.*, **575**, 230 (2006).
9. R. J. Lasheras, C. Bello-Gálvez and J. M. Anzano, Quantitative Analysis of Oxide Materials by Laser-Induced Breakdown Spectroscopy with Argon as an Internal Standard. *Spectrochim. Acta* B., **82**, 65 (2013).
10. E. C. Ferreira, J. M. Anzano, D. M. B. P. Milori, E. J. Ferreira, R. J. Lasheras, B. Bonilla, B. Montull-Ibor, J. Casas and L. M. Neto, Multiple Response Optimization of Laser-Induced Breakdown Spectroscopy Parametersfor Multi-Element Analysis of Soil Samples, *Appl. Spectrosc*., **63**, 1081 (2009).
11. J. Anzano and R. Lasheras, Strategies for the Identification of Urinary Calculus by Laser Induced Breakdown Spectroscopy, *Talanta*, **79**, 352 (2009).
12. J. M. Anzano, A. Akseli, S. J. Lehotay and J. D. Winefordner, A Comparison between Conventional and Laser Excited Fluorescence Spectrometry for the Detection of Thenoyltrrifluoroacetone-Trioctylphosphine Oxide Europium and Samarium Complexes in Hexane. *Anal. Lett*., **25**, 151 (1992).
13. A. Badiola, J. I. Canudo and G. Cuenca-Bescós, A Systematic Reassessment of Early Cretaceous Multituberculates from Galve (Teruel, Spain), *Cretaceous Res.*, **32**, 45 (2011).
14. J. I. Canudo, J. M. Gasca, M. Aurell, A. Badiola, H. A. Blain, D. Gómez-Fernández, M. Moreno-Azanza, J. Parrilla, R. Rabal-Garces and J. I. Ruiz-Omeñaca, La Cantalera: an Exceptional Window onto the Vertebrate Biodiversity of the Hauterivian-Barremian Transition in the Iberian Peninsula, *J. Iber. Geol.*, **36**, 205 (2010).
15. J. I. Canudo, J. M. Gasca, M. Moreno and M. Aurell, New Information about the Stratigraphic Position and Age of the Sauropod *Aragosaurus ischiaticus* from the Early Cretaceous of the Iberian Peninsula. *Geol. Mag*., **149**, 252 (2012).